Available online at www.sciencedirect.com
ScienceDirect
Polymer 47 (2006) 7103–7110
polymer
www.elsevier.com/locate/polymer

Unique clay orientation in the injection-molded bar of isotactic polypropylene/clay nanocomposite

Ke Wang [a], Ping Zhao [a], Hong Yang [a], Si Liang [a], Qin Zhang [a], Rongni Du [a], Qiang Fu [a,*], Zhenqiang Yu [b], Erqiang Chen [b]

[a] *Department of Polymer Science and Materials, Sichuan University, State Key Laboratory of Polymer Materials Engineering, Chengdu 610065, People's Republic of China*

[b] *College of Chemistry and Molecular Engineering, Perkin University, Beijing 100871, People's Republic of China*

Received 28 March 2006; received in revised form 29 July 2006; accepted 5 August 2006
Available online 30 August 2006

Abstract

In this article, the injection-molded bars of isotactic polypropylene/organoclay nanocomposite with different clay contents have been obtained via dynamic packing injection molding (DPIM). The oriented microstructure including layered nanoparticles and PP lamellae has been inspected through 2D-WAXS analyses along the sample thickness of the molded bars. Depending on the clay content and sample thickness, various oriented clay structures with nanoparticles uniplanar-axially oriented parallel to the surface of molded bar, or partially tumbled around the flow axis of the molded bar, or even a random orientation, could be observed. The observed orientation behavior of nanoparticles could be temporarily elucidated as the results of the sensitive response of layered nanoparticles to shear deformation and the structural recovery of clay network assisted by the electrostatic attraction existing between adjacent nanoplatelets.

Keywords: Clay orientation; Injection molding; iPP/organocaly nanocomposite

1. Introduction

In recent years, shear-induced orientation behaviors in polymer/layered silicate nanocomposites (PLSNs) have attracted much interests due to their potential contributions in improving mechanical, thermal and barrier properties. Some works focused attention on in situ ascertainment of orientation behavior of nanoclay tactoids/layers, conducted under shear flow-field, in polymer/clay nanocomposite solution [1,2], melt [3–5] and solid [6–8]. Schmidt et al. [1,2] described the orientation geometry of viscoelastic poly(ethylene oxide) (POE)-clay solution in a Couette shear cell. In such Couette shear field, an unusual orientation of nanoclay that the normal of clay surface was parallel to the vertical direction of shear cell was inspected through small angle neutron scattering (SANS) [1], furthermore, the authors proposed a physical explanation that is related to the viscoelastic properties of composite solution for the orientation of clay plates [2]. Direct evidence for shear-induced orientation in intercalated PP/organoclay nanocomposite melt was provided by Lele et al. [9]. The in situ rheo-X-ray measurements exhibited clearly that the clay tactoids could be easily oriented by shear and a large level of orientation could be achieved after a rheological yield transition from high molten viscosity to low viscosity. Interestingly, Okamoto et al. found that the surface of silicate layers aligned perpendicular rather than parallel to the stretching direction through spatially resolved TEM analysis [10], as the PP/clay nanocomposite melt was subjected to uniaxial elongation deformation.

Hierarchical microstructures with highly oriented structure including both nanoclay and polymer matrix have been three-dimensional spatially estimated in nanocomposite films of

* Corresponding author. Tel.: +86 28 85460953; fax: +86 28 85405402.
E-mail address: qiangfu@scu.edu.cn (Q. Fu).

0032-3861/$ - see front matter © 2006 Elsevier Ltd. All rights reserved.
doi:10.1016/j.polymer.2006.08.022

polyethylene/clay [11], nylon-6/clay [12,13] and triblock copolymer/clay [14,15]. Contrasting to thin film, the evaluation of oriented microstructure in injection-molded bar becomes more difficult because of the existences of a shear gradient and a temperature gradient from the skin to the core in the samples. A variety of oriented microstructures of nanoclay and polymer matrix along the thickness direction of molded bar are expected. The development of oriented microstructures from the skin to the core in the molded bars of conventional polymer/inorganic filler composites has been established in some previous studies. For such composites, the inorganic filler content was usually higher than 20 wt%. Choi and Kim [16] estimated the variation of orientation level of layered talc particles from the skin to the core in the injection-molded polypropylene/ethylene-propylene rubber/talc composite through the edge view SEM images: the surface normal of talc particle oriented almost perpendicular to the flow direction in the skin; the orientation direction of talc surface normal changed to the flow direction in the intermediate zone; while the normal of talc surface randomly oriented in the core. A triple layer structure with different preferred orientations in each region has been clearly described by Kojima et al. [17] in injection-molded nylon-6/clay composite. In the surface layer, both the plane of silicate layer and the chain axis of nylon-6 crystallite are parallel to the molded bar surface. In the intermediate layer, the plane of clay platelet remained parallel to the surface of molded bar but the chain axis of nylon-6 crystal oriented perpendicular to the plane of clay platelet. And in the core region, the silicate layers were randomly oriented around the flow axis, and the axes of nylon-6 chains were kept perpendicular to the surfaces of silicate layers. In several recent works [18–21], the development of structural hierarchy in the injection-molded bar of polymer/layered silicate nanocomposites has been carefully investigated. Though the hierarchical microstructures with a changed orientation of nanoclay and crystalline lamella of polymer matrix along the thickness direction of molded bars are very interesting and usually observed, the change of clay surface normal from the skin to the core along the sample thickness has not been fully understood so far.

It is well known that a so-called ''three-dimensional filler network structure'' will be constructed in the polymer/layered silicate nanocomposites when the content of layered clay reaches a value of threshold, at which the silicate sheets are incapable of freely rotating due to physical jamming and connecting of the nanodispersed layered silicate. One expects an increased physical jamming force of the nanodispersed silicate layers as increasing the clay content, particularly, after the formation of such filler network structure. In this work, we will demonstrate, by using iPP/organoclay nanocomposites with different clay contents as an example, a very interesting orientation and tumbling phenomenon of the clay layer from the skin to the core in the injection-molded bar. To enhance the orientation degree, dynamic packing injection molding was employed, where the melt is firstly injected into the mold and then forced to move repeatedly in a chamber by two pistons that move reversibly with the same frequency as the solidification progressively occurs from the mold wall to the molding core part. Our work indicates that the competition between the external shear force and the internal jamming force of the filler network determines the overall orientation of clay along the sample thickness.

2. Experimental

2.1. Materials

A commercially available isotactic polypropylene (trade marked as T30S, Yan Shan Petroleum China) with $M_n = 29.2\times10^3$ g/mol and a melt flow index (MFI) of 0.9975 g/min (190 °C, 2.16 kg) and a density of 0.91 g/m^3, was used as the basal polymer. The compatiblizer, PP grafted maleic anhydride (PP-MA) (MA content = 0.9 wt%, MFI = 6.74 g/min at 190 °C), was purchased from Chen Guan Co. (Sichuan, China). Sodium montmorillonite with a cation exchange capacity (CEC) of 68.8 mmol/100 g (RenShou, Sichuan, China) was organically modified through ion-exchanged reaction with dioctadecyl dimethylammonium bromide and the detailed procedure could be found in our previous publication [22]. Thereafter, the organically modified MMT was abbreviated as OMMT.

2.2. Preparation of injection-molded bars

The compatibilized nanocomposites of iPP/PP-MA/OMMT (90/10/x wt%, $x = 1,3,5,10$) were melt-mixed in a TSSJ-2S co-rotating twin-screw extruder. After pelletized and dried, composites were injected into a mold with the aid of a SZ 100 g injection-molding machine with barrel temperature of 190 °C and injection pressure of 900 kg cm^{-2}. Then dynamic packing injection molding (thereafter was abbreviated as DPIM) technology was applied. Its main feature was to introduce shear on the cooling melt during packing stage by two pistons that moved reversibly with the same frequency (1.0 Hz). The processing parameters and the characteristics and detail experimental procedure of DPIM were described in Ref. [23]. Compared with the conventional static samples which usually comprised skin zone and core zone, a triple-zone complex structure divided into skin, oriented zone and core along the depth was formed due to the temperature difference between the mold cell and the melt, and due to the oscillatory shear applied during solidification. And this triple-region structure is schematically illustrated in Sketch 1.

2.3. 2D-wide-angle X-ray scattering (2D-WAXS)

The two-dimensional wide-angle X-ray scattering experiments (2D-WAXS) were conducted using a Bruker D8 diffractometer with a GADDS 2D detector. The wavelength of the monochromated X-ray from Cu Kα radiation was 0.154 nm and reflection mode was used. For identifying both orientation structures of OMMT platelets and PP lamellae, the detected 2θ range was adjusted from 0.6° to 23°. The pieces of skin, oriented zone and core were cut apart from the injection-molded

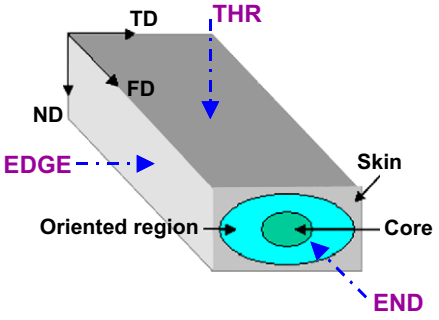

Sketch 1. Schematic illustration of triple complex structure in the dynamic injection-molded bar and spatial relationship between three irradiation planes of X-ray.

bar along the sample thickness direction. In order to obtain the 3D-analysis of orientation microstructure, the X-ray beam was irradiated on the pieces from three projection directions defined as THR, EDGE and END, as shown in Sketch 1. Meanwhile, in Sketch 1, FD, TD and ND represent the flow direction, the transverse direction and the normal direction, respectively.

3. Results and discussion

As a typical example, the oriented behaviors of OMMT particles and PP lamellae of iPP/OMMT nanocomposite (5 wt% OMMT) in various regions of dynamic bar have been demonstrated through 2D-WAXS analyses in the 3D spacing, as shown in Fig. 1. FD is vertical in the THR view and EDGE view, TD is horizontal in the THR view and END view, and ND is horizontal in the EDGE view whereas is vertical in the END view. Furthermore, the integrated intensity vs. 2θ patterns and the azimuthal scans of OMMT (001) plane are also plotted in Figs. 2 and 3, respectively, to quantitatively evaluate the variation of OMMT orientation along the depth of molded bar. Within the skin region, a pair of tri-level spots near the stopper, representing the *d*-spacing of OMMT stacks, focus on the equator of EDGE view and the meridian of END view. In the THR view, on the other hand, no obvious reflection corresponding to the ordered stacking of OMMT particles can be observed. These scattering characteristics suggest that a high degree ordering of assembly of OMMT tactoids along the FD has formed in the skin, which is a uniplanar-axial orientation of OMMT tactoid with the tactoid surface parallel to the molded bar surface (FD–TD plane). Such uniplanar-axial orientation of layered silicate seems to be easily formed in the presence of intensive shear and dramatic temperature gradient and has also been found in the nanocomposite films [12,24,25] and some other injection-molded composites [17,26]. To quantify the difference of OMMT scattering intensity between the EDGE view and the THR view, it should be noted that the maximal intensity of OMMT tactoids in the

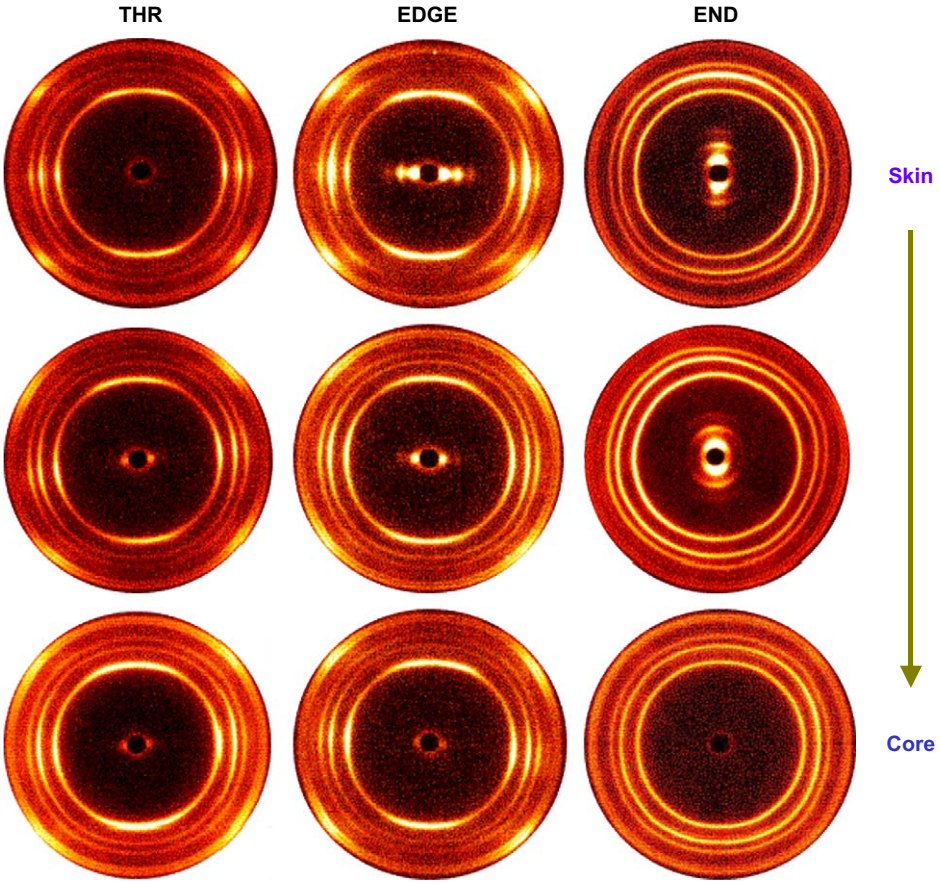

Fig. 1. 2D-WAXS patterns illustrate the spatially oriented microstructure in the dynamic injection-molded bar of iPP/OMMT nanocomposite (5 wt% OMMT).

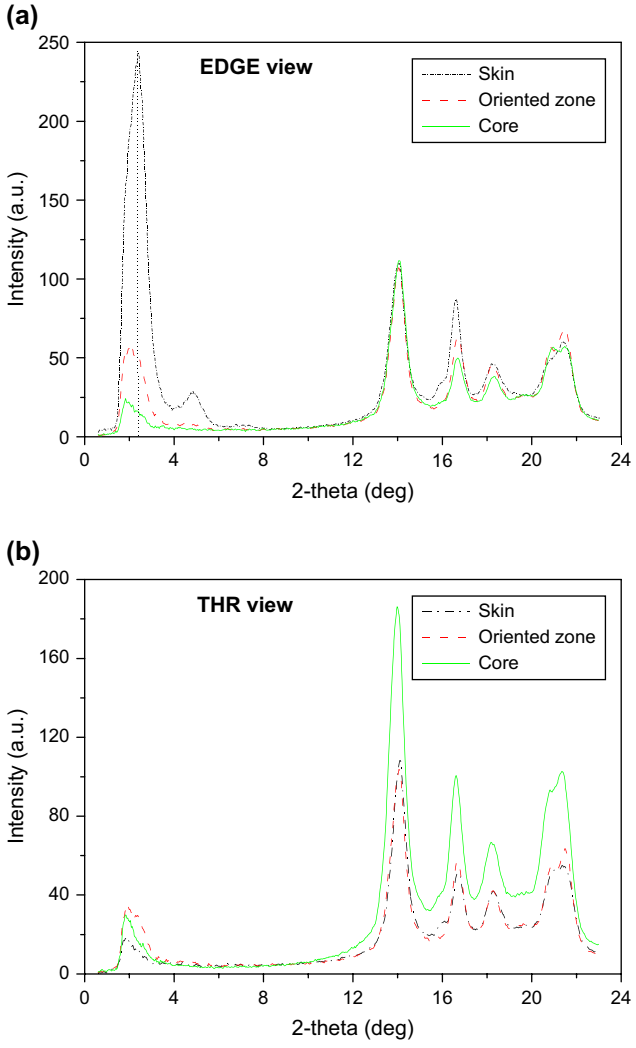

Fig. 2. Intensity vs. 2θ patterns at various regions of the dynamic injection-molded bar of iPP/OMMT nanocomposite (5 wt% OMMT): (a) EDGE view; (b) THR view.

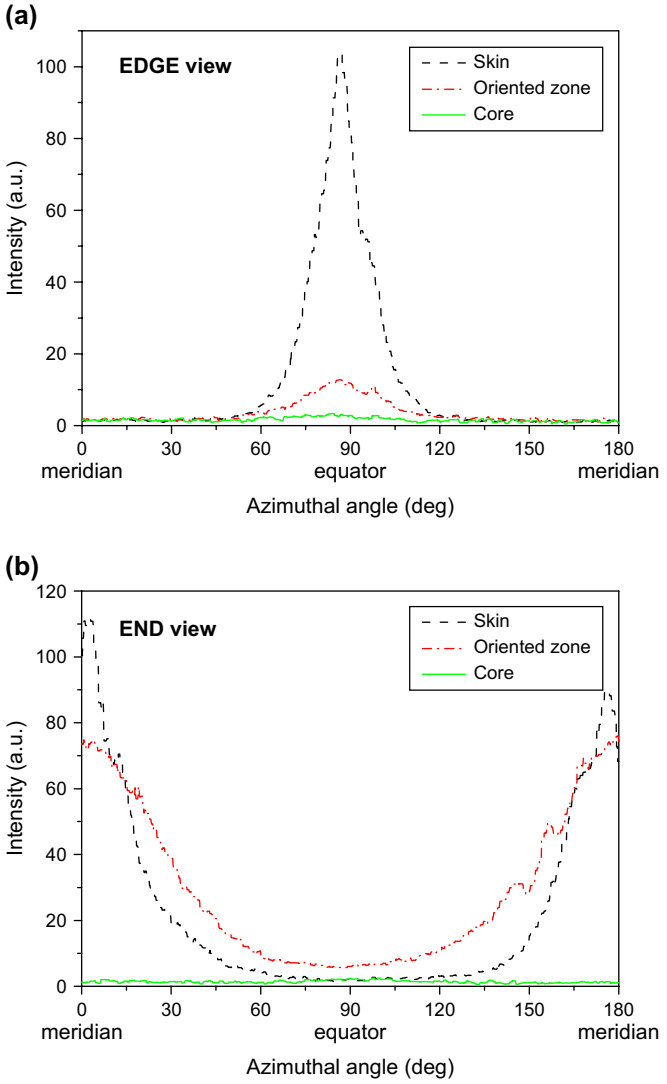

Fig. 3. Azimuthal scans of OMMT (001) plane (2θ within 1.5°–3.6°) in the dynamic injection-molded bar of iPP/OMMT nanocomposite (5 wt% OMMT): (a) EDGE view; (b) END view.

EDGE view is 14 times higher than that in the THR view, which can be calculated through comparing with the peak intensities located at about $2\theta = 2.3°$ between Fig. 2(a) and (b). In the oriented zone, a pair of intensive spots emerge on the equator of THR and EDGE images, correspondingly, a pair of broaden streaks appear on the meridian of END image. The azimuthal scans of OMMT (001) plane in the EDGE view and the END view are presented in Fig. 3(a) and (b), respectively. The half width at maximum height (HWMH) in azimuthal scanning pattern could be regarded as a criterion to evaluate the orientation level [25], whose value increase implied a decrease of orientation degree. For the EDGE view, the HWMH of peak located at 90° azimuth (equator) changes from 9.5° in the skin to 14.1° in the oriented zone; whereas, a remarkable increase of HWMH of peak located at 0° azimuth (meridian) from the skin to the oriented zone is detected in the END view, which changes from 13.1° to 30.5°. In the EDGE view, the ordering level of OMMT alignment somewhat decreases from the skin to the oriented zone, implying that the preferential orientation of OMMT tactoids parallel to the flow direction can be maintained within the oriented zone. On the other hand, the ordering degree of OMMT assembling in the END view decreases significantly from the skin to the oriented zone, thus a random alignment of OMMT nanoparticles within the oriented zone is observed. This indicates a different oriented structure of OMMT tactoid in this zone compared with that in the skin: the planes of some OMMT tactoid have tumbled around the flow axis of the molded bar, simultaneously, remained preferentially oriented along the flow direction. The core is formed at last after the cessation of shear, where the melt is freely cooled down and relaxed, thus a random orientation of tactoid is expected in the plane perpendicular to the shear flow direction. It should be noted that the intensity of *d*-spacing reflection of OMMT tactoids is very weak in the core. The reflection intensity of OMMT becoming feint doesn't come from inhomogeneous distribution of OMMT along the depth of molded bar because the contents of inorganic filler ash at various regions, obtained after heating the pieces of composite samples at 600 °C for

1 h, are almost equal. In one of our publications [23], we found that the exfoliation level of OMMT tactoids was considerably increased from the skin to the core in the dynamic molded bar through combination of WAXD and TEM analyses. And the enhanced exfoliation level was attributed to the gradually increased viscosity of the melt during solidification that occurred from the cold wall to the core. Almost complete exfoliation has been evidenced in this core. Thus the number of residual tactoid contributing to the intensity of spot nearby the stopper is significantly decreased, resulting in a weak intensity of reflection. By careful examination, a pair of spots focused on the equator of THR and EDGE patterns still can be recognized, indicating that OMMT nanoparticles are still preferentially oriented parallel to the flow direction with turning their surfaces around the flow axis in the core. As shown in Fig. 2, the peak area of OMMT tactoids dramatically decreases from the skin to the core in the EDGE view; nevertheless, in the THR view, such area in the core is larger than that in the skin, indeed suggesting that the tumbling of OMMT planes around the flow axis can take place even in the core.

As to the PP lamellae, in the THR and EDGE images, the intensive arcs of (110) reflection of PP α-modification, located at $2\theta = 14.1°$, emerge at both equator and meridian, and the streaks of (040) reflection, located at $2\theta = 16.9°$, only exist at the equatorial direction in the whole dynamic sample. The oriented level is, however, gradually decreased from the skin to the core. To approve this statement, the azimuthal scans of (110) plane of α-modification in the EDGE view are shown in Fig. 4. The HWMH of peak located at 90° azimuth (equator), which represents the crystal of *a**-axes orientation fraction, is increased from 9.8° for the skin to 13.3° for the oriented zone and to 17.5° for the core. The origins of the gradually decreased orientation level from skin to the core are related to shear velocity during injection molding, temperature gradient, relaxation kinetics of macromolecules, etc. and need more profound investigations. Meanwhile only isotropic reflection circles can be observed in the END images along the whole sample thickness. According to the spatially resolved 2D-WAXS analyses, the oriented microstructure of iPP crystal can be described as anisotropic cylinder within the whole molded bar. This cylindrical structure consists of such lamellae whose *a**- and *c*-axes are parallel to the long axis of cylinder (the flow direction) and *b*-axes, acted as the growth axes of lamellae, randomly rotate around the flow axis and align perpendicular to the same axis. Such biaxial orientation of iPP lamella is prevailing when iPP crystallized under shear or extension flow [24,26], and its formation mechanism has been elucidated by Fujiyama et al. [27]. It is also valuable to note that no correlation between the orientation of OMMT tactoids and the orientation of iPP lamellae has been detected in the nonpolar polyolefin/OMMT system. Otherwise, in some polar polymer/clay system, such as nylon/clay nanocomposites, the lamellae can grow perpendicular to the surface of clay particles through epitaxial growth [28] or transcrystallization [29]. Up to now, the hierarchical structure of orientations including OMMT platelets and PP lamellae in the dynamic molded bar has been demonstrated clearly and is schematically denoted in Sketch 2, which includes: (1) the

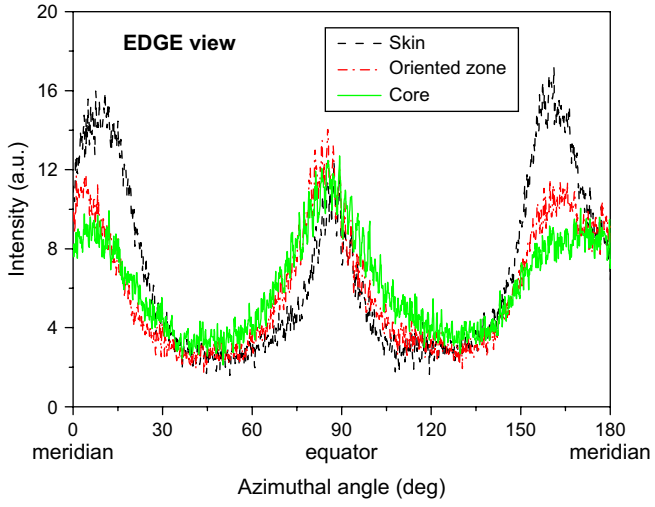

Fig. 4. Azimuthal scans of PP-crystal (110) plane (2θ within 13.4°–14.7°) in the dynamic injection-molded bar of iPP/OMMT nanocomposite (5 wt% OMMT).

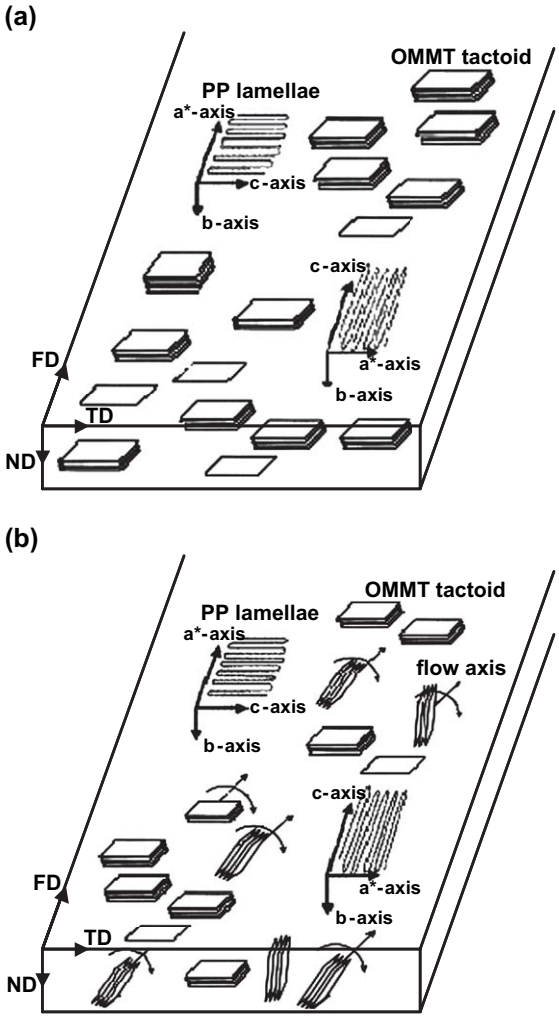

Sketch 2. 3D schematic illustrations of (a) uniplanar-axial orientation of OMMT tactoids in the skin; (b) partial tumbling of OMMT tactoids around the flow axis in the oriented zone and the core of dynamic molded bar.

uniplanar-axial orientation of OMMT tactoid with the tactoid surface parallel to the molded bar surface (FD–TD plane) in the skin; (2) the tumbling of partial OMMT planes around the flow axis in the oriented zone and the core; (3) the biaxial orientation of PP lamellae within the whole thickness of molded bar.

The mechanism of the unique orientation behavior of OMMT nanoparticles in the molded bar can be temporarily ascribed to the sensitive response of layered nanoparticles to the shear [9] and the unusual recovery of clay network after shear deformation. The layered nanoparticles with high aspect ratio can easily take preferential orientation under shear field that the surface normal is parallel to the shear velocity. While the shear gradient will induce various flow layers with different rates, the layered particle is difficult to exist simultaneously in several flow layers with different rates and would rather to choose alignment parallel to an individual flow layer. Meanwhile the melt in skin is immediately solidified after injection molding because of the dramatic temperature difference between the cold molded wall and the hot melt. Consequently, the uniplanar orientation of layered OMMT particles is reserved in the skin. In the internal parts, including the oriented zone and the core, the relaxation of preferentially aligned nanoparticles will occur more or less. What is the essential factor determining the observed relaxation of oriented nanoplatelets in the molded bar? As mentioned above, a so-called clay network can be constructed when the content of layered clay reaches a threshold value of physical correlation, at which the silicate sheets are incapable of freely rotating due to physical jamming and connecting. It has been generally accepted that silicate sheets possess positively charged edges and negatively charged faces [30,31]. When the percolated clay network is formed, the individual sheets will connect with each other through electrostatic attraction. As to our speculation, such electrostatic attraction will be responsible for the structural recovery of clay network destroyed under shear deformation. Additionally, it should be mentioned that the structural relaxation of nanocomposite melt after cessation of shear could be ascertained by dynamic rheometry, and the detail description and relevant experimental results will be published in our next paper [32].

The change of clay content in PP matrix will result in different dispersion morphologies of clay nanoparticles, thus induce different levels of internal physical jamming force and structural recovery capability of clay network. According to the rheological studies, the percolated clay network would make the polymer/clay melt to exhibit pseudo-solidlike rheological properties. In our work [32], the pseudo-solidlike rheological response has been detected in the composites with higher clay content (more than 5 wt%). For iPP/OMMT nanocomposite with lower clay content, the correlation between clay sheets was weak and the clay network couldn't be easily formed. Unlike the case of 5 wt%, in the oriented zone of dynamic bar of nanocomposite containing 1 wt% and 3 wt% OMMT, no or very weak relaxation of uniplanar-axially oriented OMMT sheets tumbling around the shear flow axis is detected. The spots representing the ordering stack of OMMT layers are only visible in the EDGE view, as shown in Fig. 5. Therefore, it can be considered: before the formation of clay network, very limited interaction exists between clay nanoplatelets, resulting in a slow kinetics of relaxation of oriented clay nanoplatelets originated by shear deformation; whereas, after the formation of clay network, the electrostatic attraction existing between adjacent clay sheets will aid the relaxation and turning of uniplanar-axially oriented sheets and accelerate the kinetics of structural recovery of clay network. At this moment, it is not clear why the tumbling opposite to the shear axis or around the TD axis is intensively depressed, which may be related to the complicated mechanical geometry and processing thermal history. So further investigation is needed.

On the other hand, with the increasing content of OMMT, a significantly larger physical correlation of clay network is expected and the interaction between OMMT nanoplatelets becomes strong. It will dissipate more energy for breaking the physical jamming and electrostatic attraction between clay platelets at high OMMT content than that with low clay content. As an example, 2D-WAXS patterns of the skin in iPP/OMMT nanocomposite containing 10 wt% OMMT are presented in Fig. 6. Compared with the sample containing 5 wt% OMMT, a pair of spots located at the image center are seen in the THR view and two broaden streaks lie on the meridian of END view, indicating that the physical jamming and electrostatic attraction between adjacent nanoparticles have greatly hindered the tumbling and orientation of nanoparticles under the shear flow. Thus OMMT sheets are not totally oriented parallel to the surface of molded bar even in the skin and a low degree of preferential orientation of OMMT is observed in the TD–ND plane. For clear purpose and

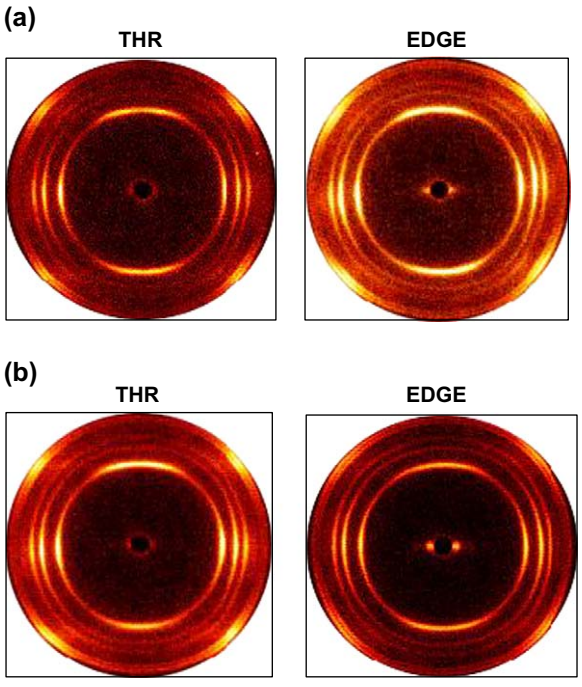

Fig. 5. 2D-WAXS patterns in the oriented zones of the injection-molded bars containing (a) 1 wt% OMMT; (b) 3 wt% OMMT.

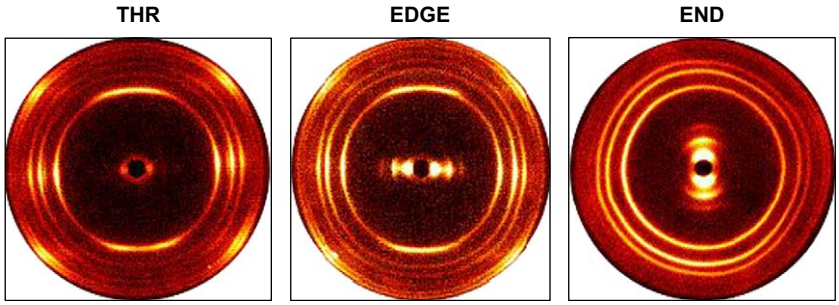

Fig. 6. 2D-WAXS patterns illustrate the spatially oriented microstructure of skin in the dynamic injection-molded bar of iPP/OMMT nanocomposite (10 wt% OMMT).

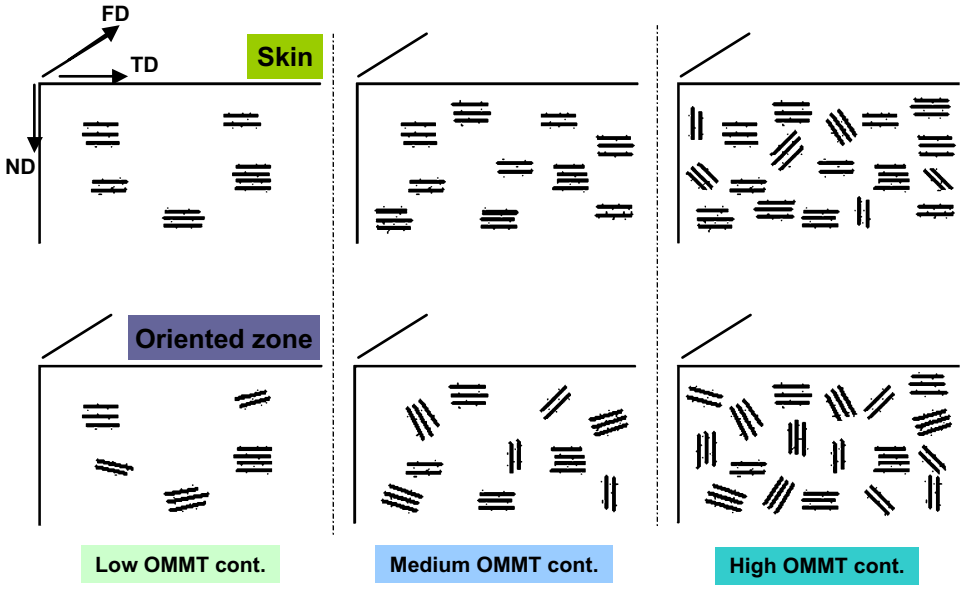

Sketch 3. Schemes represent the orientation of OMMT tactoids within different regions of molded bar at low, medium and high OMMT contents.

facilitation, various orientations of OMMT platelets within different regions at different contents, are schematized in Sketch 3. One may note that the gradual decrease of the ordering level of OMMT platelets in the END view depends on the increase of OMMT content and the depth of molded bar.

4. Conclusions

A unique oriented microstructure in the molded bar of iPP/OMMT nanocomposite has been ascertained clearly through spatially resolved 2D-WAXS analyses. When the clay content is low, nanoparticles are found to be uniplanar-axially oriented parallel to the surface (FD–TD plane) of molded bar along the whole depth. With increasing the clay content, although the preferential orientation of nanoparticles along the flow direction is still kept in the oriented zone, a partial tumbling of layered clay around the flow axis of the molded bar is observed. When the content of clay is higher, only a low degree of preferential orientation can be observed even in the skin. The observed orientation behavior of OMMT nanoparticles in the injection-molded bars can be temporarily elucidated as the results of the sensitive response of layered nanoparticles to shear deformation and the structural recovery of clay network assisted by the electrostatic attraction existing between adjacent OMMT nanoplatelets. A competition between the external shear field and the internal jamming force of filler particles and the kinetics of structural recovery of clay network determines whether the preferential orientation of clay sheets takes place or not during shear process, and then maintains oriented state or adopt partial relaxation after cessation of shear.

Acknowledgements

We would like to express our great thanks to the National Natural Science Foundation of China for financial support (20404008, 50533050, 50373030 and 20490220). This work is subsidized by the special funds for Major State Basic Research Projects of China (2003CB615600) and by Ministry of Education of China as a key project (104154).

References

[1] (a) Schmidt G, Nakatani AI, Butter PD, Karim A, Han CC. Macromolecules 2000;33:7219;

(b) Schmidt G, Nakatani AI, Butter PD, Han CC. Macromolecules 2002;35:4725.
[2] (a) Lin-Gibson S, Kim H, Schmidt G, Han CC, Hobbie EK. J Colloid Interface Sci 2004;274:515;
(b) Lin-Gibson S, Schmidt G, Kim H, Han CC, Hobbie EK. J Chem Phys 2003;119:8080.
[3] Krishnamoorti R, Giannelis EP. Macromolecules 1997;30:4097.
[4] Ren JX, Silva AS, Krishnamoorti R. Macromolecules 2003;33:3739.
[5] Krishnamoorti R, Giannelis EP. Langmuir 2001;17:1448.
[6] Kim JH, Koo CM, Choi YS, Wang KH, Chung IJ. Polymer 2004; 45:7719.
[7] Wang KH, Chung IJ, Jang MC, Keum JK, Song HH. Macromolecules 2002;35:5529.
[8] Dai XH, Xu J, Guo XL, Lu YL, Shen D, Zhao N, et al. Macromolecules 2004;37:5615.
[9] Lele A, Mackley M, Galgali G, Ramesh C. J Rheol 2002;46:1091.
[10] Okamoto M, Nam PH, Maiti P, Kotaka T, Hasegawa N, Usuki A. Nano Lett 2001;1:259.
[11] Bafna A, Beaucage G, Mirabella F, Mehta S. Polymer 2003;44:1103.
[12] Park SY, Chi YH, Vaia RA. Macromolecules 2005;38:1729.
[13] Medellin-Rodriguez FJ, Burger C, Hsiao BS, Chu B, Vaia R, Phillisps S. Polymer 2001;42:9015.
[14] Ha YH, Kwon Y, Breiner T, Chan EP, Tzianetopoulou T, Cohen RE, et al. Macromolecules 2005;38:5170.
[15] Lee JY, Park MS, Yang HC, Cho K, Kim JK. Polymer 2003;44:1705.
[16] Choi WJ, Kim SC. Polymer 2003;45:2393.
[17] Kojima Y, Usuki A, Kawasumi M, Okada A, Kurauchi T, Kamigaito O, et al. J Polym Sci Part B Polym Phys 1995;33:1039.
[18] Yuan M, Turng LS. Polymer 2005;46:7273.
[19] Konishi Y, Cakmak M. Polymer 2005;46:4811.
[20] Yalcin B, Cakmak M. Polymer 2004;45:2691.
[21] Yui H, Wu G, Sano H, Sumita M, Kino K. Polymer 2006;47:3599.
[22] Zhang Q, Wang K, Men Y, Fu Q. Chin J Polym Sci 2003;21:359.
[23] Wang K, Liang S, Zhang Q, Fu Q. J Polym Sci Part B Polym Phys 2005;43:2005.
[24] Koo CM, Kim JH, Wang KH, Chung IJ. J Polym Sci Part B Polym Phys 2005;43:158.
[25] Malwitz MM, Lin-Gibson S, Hobbie EK, Butler PD, Schmidt G. J Polym Sci Part B Polym Phys 2003;42:3237.
[26] Fujiyama M, Wakino T. J Appl Polym Sci 1991;42:9.
[27] Fujiyama M, Wakino T, Kawasaki Y. J Appl Polym Sci 1988;35:29.
[28] Maiti P, Okamoto M. Macromol Mater Eng 2003;288:440.
[29] Kim GM, Lee DH, Hoffmann B, Kressler J, Stoppelmann G. Polymer 2001;42:1095.
[30] Krishnamoorti R, Silva AS. In: Pinnavaia TJ, Brall GW, editors. Polymer–clay nanocomposites. New York: John Wiley & Sons; 2000. p. 315–43.
[31] Haraguchi K, Li HJ, Matsuda K, Takehisa T, Elliott E. Macromolecules 2005;38:3482.
[32] Wang K, Liang S, Deng J, Yang H, Zhang Q, Fu Q, et al. The role of clay network on macromolecular chain mobility and relaxation in isotactic polypropylene/organoclay nanocomposites. Polymer, in press, doi:10.1016/j.polymer.2006.07.067.